Inorganic Chemistry

pubs.acs.org/IC

Article

Isocyanate Insertion into a La−P Phosphide Bond: A Versatile Route to Phosphaureate-Bridged Heterobimetallic Lanthanide−Coinage-Metal Complexes

Fabian A. Watt, Nicole Dickmann, Roland Schoch, and Stephan Hohloch*

Cite This: *Inorg. Chem.* 2020, 59, 13621−13631

Read Online

ACCESS | Metrics & More | Article Recommendations | Supporting Information

ABSTRACT: A new route to heterobimetallic lanthanide−coinage-metal complexes is disclosed. The selective insertion of organic substrates such as phenyl iso(thio)cyanate into the La−P bond of the primary phosphido complex **(PN)$_2$La(PHMes)** (**1**) (with PN$^-$ = (*N*-(2-(diisopropylphosphanyl)-4-methylphenyl)-2,4,6-trimethylanilide) yields the phospha(thio)ureate complexes **(PN)$_2$La(OC(NPh)(PHMes))** (**2**) and **(PN)$_2$La(SC(NPh)(PHMes))** (**3**) with retention of the P*H* protons. Subsequent deprotonation of the phosphaureate complex **2** with potassium hexamethyldisilazide (KHMDS, K[N(SiMe$_3$)$_2$]) leads to the polymeric complex **[K{(PN)$_2$La(OC(NPh)(PMes))}]$_n$** (**4**). Complex **4** was found to be an excellent precursor for salt metathesis reactions with copper(I) and gold(I) chlorides supported by an N-heterocyclic carbene (NHC, **5** and **6**) or a cyclic alkyl amino carbene (CAAC, **7** and **8**). This resulted in the unprecedented formation of heterobimetallic lanthanum−coinage-metal complexes, containing the first example of a $\mu,\kappa^2(O,N):\kappa^1(P)$-phosphaureate bridging ligand. For an alternative route to complex **8** a direct protonolysis protocol between a new basic gold(I) precursor, namely **(^{Me}CAAC)Au(HMDS)**, and **2** was also investigated. The complexes have been characterized by multinuclear NMR spectroscopy, IR spectroscopy, and X-ray crystallography (except for **8**).

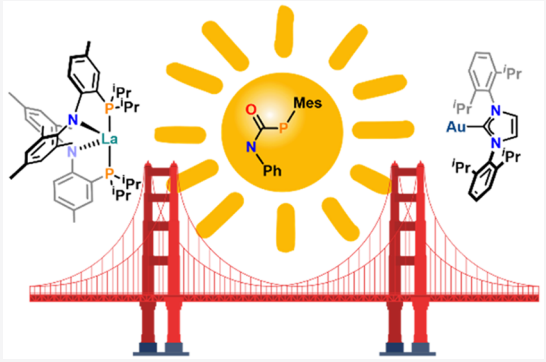

INTRODUCTION

The chemistry of the lanthanides (Ln) has advanced to be a very important field of research in modern inorganic chemistry.[1,2] As lanthanides are well-known for their magnetic and luminescent properties, the applications of lanthanide-containing molecules range from molecular magnetism[3−11] and (bio)analytical sensors[12−14] to optical communication[15] and modern catalysis.[16−31] In recent years, new strategies to systematically analyze and design lanthanide complexes with the desired chemical, magnetic, or photophysical properties have emerged.[4,6,32−35] In this context, transition metals such as iron(0/II/III),[36−43] nickel(II),[44−47] and zinc(II)[45,48,49] have been used to influence the magnetic behavior of lanthanide compounds, whereas e.g. iridium(III),[50] rhenium(I),[51] platinum(II),[51−54] palladium(II),[54] zinc(II),[48,55] gold(I),[54,56,57] and silver(I)[54] have been introduced for efficient sensitizing of lanthanide luminescence[58−60] in heterobimetallic or -trimetallic systems. Despite these significant advances, straightforward and rational designs of heterobimetallic lanthanide−coinage-metal complexes in particular have not been much developed as yet.

Early-transition-metal and f-element phosphido complexes are known to show a rich insertion chemistry which is very useful for the construction of exotic and rare types of phosphorus-containing ligands directly at the metal ion. A considerable number of examples have been reported by the groups of Hey-Hawkins and Stephan in the 1990s and include, for instance, phosphaguanidinates,[63] phospha(thio)ureates[64] and phosphaamidinates[65,66] at zirconium(IV). In recent years, more examples of analogous lanthanide and actinide (Ac) complexes have accumulated.[28,31,61,62,67−73] From a thermodynamic point of view, the favorable exchange of rather weak M−P bonds for more ionic M−N or M−O bonds provides the main driving force in these processes.[23] The insertion of carbodiimides, iso(thio)cyanates, and nitriles as well as alkynes and olefins into Ln−P (or Ac−P) bonds is also considered a crucial elementary step in lanthanide (or actinide)-catalyzed hydrophosphin(yl)ation reactions.[26−31,62,74] The complexes which are intermediately formed in these catalytic cycles can often be isolated and characterized in separate stoichiometric experiments (Figure 1).[28,31,61,62]

To date, in the case of lanthanide complexes diphenylphosphanyl-substituted insertion products have been investigated

Received: July 3, 2020
Published: September 4, 2020

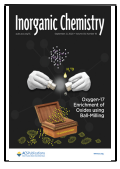

https://dx.doi.org/10.1021/acs.inorgchem.0c01971
Inorg. Chem. 2020, 59, 13621−13631

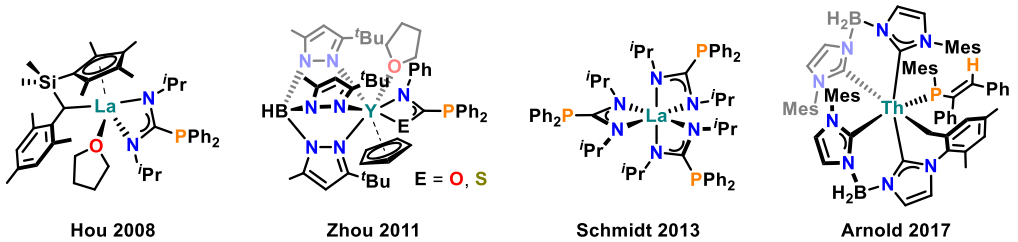

Figure 1. Selection of isolated insertion products of lanthanide and actinide phosphido complexes.[28,31,61,62]

almost exclusively, leaving no possibility for further functionalization of the newly formed coordinated ligand. Still, there is one example in the literature of functionalizing related guanidinate ligands at the pnictogen (N) atom in the first coordination sphere of lanthanide ions (Scheme 1).[75] This

Scheme 1. Functionalization of a Guanidinate Ligand in the First Coordination Sphere of Lanthanide Ions (R = Me, ^{t}Bu[75])

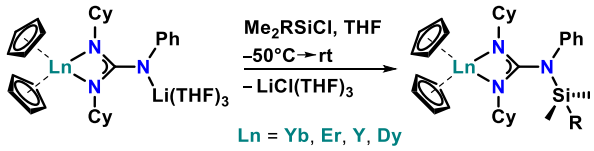

report by Zhou and co-workers from 2010 showed that heterobimetallic lanthanide−lithium complexes, obtained by deprotonation of coordinated guanidinate with *n*-butyllithium, can be selectively silylated. However, the authors did not further investigate transmetalation reactions to obtain other, more interesting heterobimetallic systems.

In 2018, Walensky and co-workers presented the addition of *tert*-butylnitrile across one of the Th−P bonds of a thorium(IV) bis(mesitylphosphido) complex with concurrent proton transfer from phosphorus to nitrogen (Scheme 2).[68] Intriguingly, the newly formed phosphaamidinate ligand could be selectively deprotonated by a strong base such as KHMDS in the presence of 2,2,2-cryptand, resulting in a rare example of an end-on-coordinated dianionic aza-1-phosphaallyl ligand.

Recently, our group has reported the synthesis of primary phosphido complexes **(PN)$_2$Ln(PHMes)** (Ln = La, Lu) supported by a bidentate, monoanionic anilidophosphine ligand (*N*-(2-(diisopropylphosphanyl)-4-methylphenyl)-2,4,6-trimethylanilide, abbreviated PN$^-$).[76] Intrigued by the examples of Walensky[68] and Zhou,[75] we were interested if our complex **(PN)$_2$La(PHMes)** (**1**) is prone to undergo a similar insertion chemistry with heterocumulenes. This type of reactivity has already been reported for group IV and actinide primary phosphido complexes[64,71] but is virtually nonexistent for lanthanides. We envisioned that retention of the P*H* proton after insertion might be a valuable tool to obtain further reactivity: i.e., deprotonation and subsequent metalation with late-transition-metal complexes. In the following, we will describe the successful application of this strategy to obtain new types of heterobimetallic lanthanum−copper(I) and lanthanum−gold(I) complexes.

RESULTS AND DISCUSSION

On consideration of the NMR spectroscopic advantages of diamagnetic lanthanum(III) compounds and the straightforward multigram-scale synthesis of the respective chloride precursor complex,[76] the primary phosphido complex **1** was chosen as the starting point for the evaluation of our targeted synthesis route. The first step of the reaction sequence, namely the insertion of either phenyl isocyanate or phenyl isothiocyanate into the La−P phosphide bond in **1** (Scheme 3), was found to proceed quickly at room temperature. This was indicated by an immediate color change from deep yellow to pale yellow during the addition of 1 equiv of phenyl iso(thio)cyanate.

The reactions could be easily monitored by ^{31}P NMR spectroscopy, showing that within minutes full and clean conversion to a new complex had occurred in both cases. Removal of toluene *in vacuo* followed by trituration and washing with *n*-hexane or *n*-pentane gave an analytically pure product as an off-white (**2**) or pale yellow (**3**) powder in good isolated yields (>80%), respectively. Like the phosphido complex **1**, the ^{31}P NMR spectra of the new complexes **2** and **3** in C_6D_6 show one singlet resonance for two chemically equivalent PN ligands as well as a doublet resonance for the PHMes moiety in a ratio of 2:1. A pronounced high-field shift of the *P*HMes doublet resonance from δ −36.4 ppm (**1**) to δ −90.1 and −56.4 ppm for **2** and **3**, respectively, indicated the successful insertion of phenyl iso(thio)cyanate. Similar ^{31}P shifts upon insertion of various iso(thio)cyanates into Zr−PHR (R = Cy, 2,4,6-^{i}Pr$_3$C$_6$H$_2$) bonds have been reported earlier.[64] Additionally, the large doublet splittings of 242.8 and 242.4 Hz magnitudes for **2** and **3**, respectively, lie in the typical range of $^1J_{PH}$ coupling constants.[64,69,76−78] These couplings disappear in the ^{31}P{^{1}H} NMR spectra to give singlet

Scheme 2. Insertion of *tert*-Butylnitrile into a Th−P Bond of a Thorium(IV) Bis(mesitylphosphido) Complex, Followed by Deprotonation of the Phosphaamidinate Ligand[68]

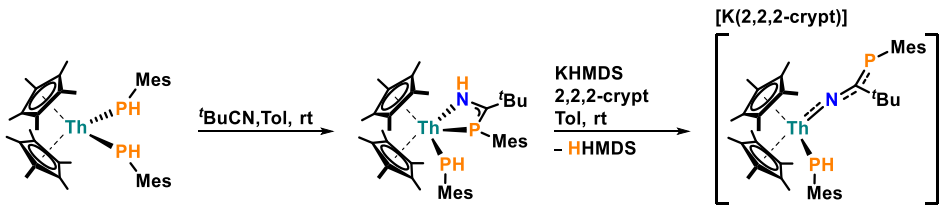

https://dx.doi.org/10.1021/acs.inorgchem.0c01971
Inorg. Chem. 2020, 59, 13621−13631

Scheme 3. Insertion of Phenyl Isocyanate or Phenyl Isothiocyanate into the La−P Phosphide Bond of 1, Yielding Phospha(thio)ureate Complex 2 or 3

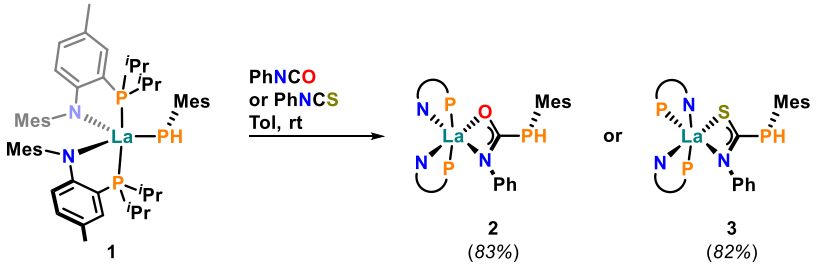

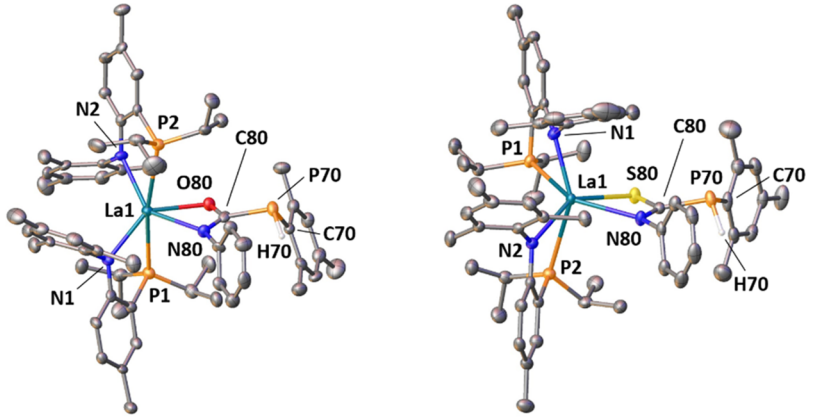

Figure 2. Thermal ellipsoid plots of **2** (left) and **3** (right). Thermal ellipsoids are shown at a probability level of 30%. Hydrogen atoms (except for H70) and solvent molecules have been omitted for clarity.

resonances, unambiguously confirming the retention of the P*H* proton. Likewise, the PN ligand resonances of **2** and **3** are also shifted to high fields (δ 6.3 ppm (**2**) and 6.9 ppm (**3**) compared to δ 11.0 ppm for **1**). This is in agreement with an increase in the coordination number at lanthanum(III) by +1 and a diminished degree of donation from the $^{i}Pr_2$-phosphanyl groups to the lanthanum atom after insertion. In the corresponding ^{1}H NMR spectra, the presence of a new set of aromatic resonances due to the introduced phenyl substituent as well as significant low-field shifts of the P*H* resonance from δ 3.42 ppm for **1** to δ 5.11 and 5.32 ppm for **2** and **3**, respectively, can be considered as additional indicators of successful phospha(thio)ureate formation. Finally, the expected connectivity was further confirmed by $^{13}C\{^{1}H\}$ NMR spectroscopy, with new resonances at low fields of δ 186.5 ppm (**2**) and 208.0 ppm (**3**) for the PhNCX quaternary carbon atom of the inserted iso(thio)cyanate fragment (X = O, S). The observed doublet splitting of 35 Hz magnitude in the case of **2** results from $^{1}J_{CP}$ coupling to the adjacent *P*HMes phosphorus atom and compares very well to reported literature values.[64]

Unambiguous structural proof for the formation of insertion products **2** and **3** was obtained by X-ray diffraction studies (Figure 2). X-ray-quality crystals were obtained by either storing a concentrated solution of **2** in a mixture of *n*-hexane and a minimal amount of toluene obtained during workup or gas diffusion of *n*-hexane into a C_6D_6 solution of **3**, at room temperature, respectively. Complex **2** crystallizes in the monoclinic space group $P2_1/n$ with half a molecule of *n*-hexane in the asymmetric unit, while complex **3** was found to crystallize in the triclinic space group $P\bar{1}$ without solvent molecules in the lattice.

In both cases, the lanthanum atom is six-coordinate in a strongly distorted octahedral, almost trigonal prismatic fashion[28] by two PN ligands as well as the nitrogen and chalcogenide atoms of the newly formed phospha(thio)ureate ligand. Complex **2** exhibits a *trans* arrangement of the $^{i}Pr_2$-phosphanyl groups (P1−La1−P2 angle of 170.40(4)°), with the inserted PhNCO fragment being roughly perpendicular to it (P1/2−La1−O80 and P1/2−La1−N80 angles between 80.08(1) and 95.40(1)°, respectively). Interestingly, in the case of **3** the phosphanyl groups are *cis* to each other (P1−La−P2 angle of 82.80(6)°), indicating a high flexibility of the PN ligands for rearrangement around the lanthanum atom. While the La1−N80 distances to the phospha(thio)ureate ligand of 2.616(5) and 2.646(3) Å in **2** and **3**, respectively, are slightly larger in comparison to the average La1−N1/N2 distances of around 2.41 and 2.45 Å, both La1−N80 and La1−O80/S80 distances (2.448(4) and 2.972(2) Å, respectively) are only somewhat larger (0.05−0.2 Å) than those in related lanthanide phosphido insertion products.[28,31,61] We attribute these minor differences to slightly different ionic radii as well as the high steric demand of the two PN supporting ligands.[76] The N80−La1−O80/S80 angles of 52.2(1) and 55.57(6)° are only slightly more acute than reported angles in related Zr(IV) phospha(thio)ureate complexes.[64] The new C80−P70 bond in **2**/**3** has a length of 1.856(6) Å/1.865(3) Å, and the XCNP core (X = O, S) of the phospha(thio)ureate ligand is found to be essentially planar with sums of angles around C80 of ∼359.7 and ∼359.1°, respectively. In summary, all these structural parameters lie in the expected range for phospha(thio)ureates in the coordination sphere of highly electropositive metal ions.[61,64] Additional information on the

https://dx.doi.org/10.1021/acs.inorgchem.0c01971
Inorg. Chem. 2020, 59, 13621−13631

Scheme 4. Deprotonation of Complexes 2 and 3 with KHMDS

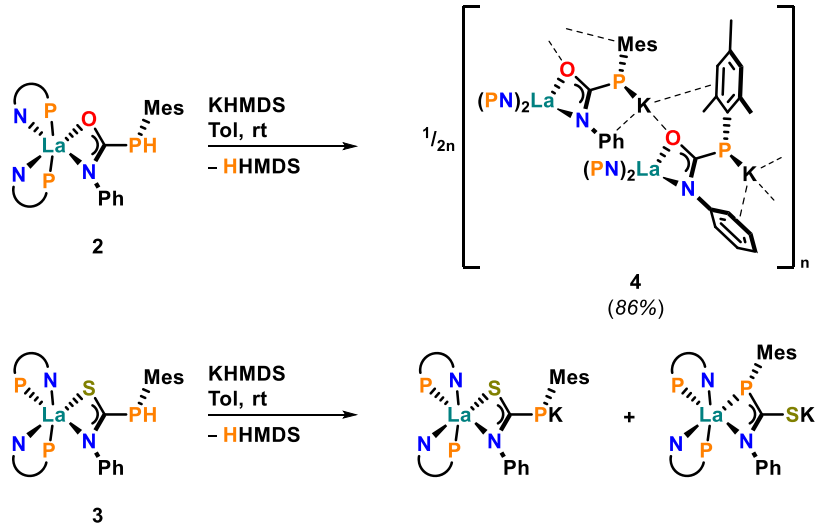

Scheme 5. Salt Metatheses of 4 with a Selection of Carbene Coinage-Metal Chlorides to Yield Complexes 5−8

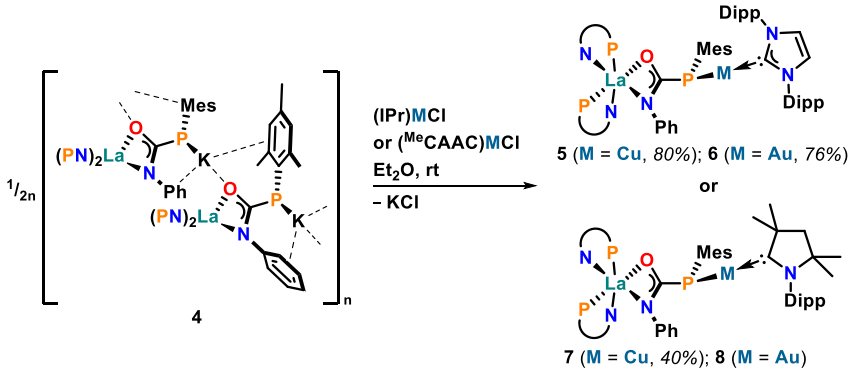

crystallographic data of **2** and **3** can be found in Tables S1 and S2 in the Supporting Information.

After having accomplished the construction of phospha-(thio)ureate ligands in the coordination sphere of PN-supported lanthanum(III), we investigated the possibility of deprotonating the *PH* group in **2** and **3**. For this purpose, complex **2** was treated with 1 equiv of KHMDS in toluene[79] at room temperature (Scheme 4, top). The initially yellow solution turned into a thick yellow suspension overnight. Clearly, this indicated the formation of a discrete salt or coordination polymer, since all other lanthanum complexes up to this point were readily soluble in toluene or benzene and the related potassium salt of the PN ligand (**KPN**) is also known to crystallize from concentrated aromatic solvents (i.e., C_6D_6).[76] This notion was substantiated by the fact that the isolated material of the new compound **4** could only be dissolved in a coordinating solvent such as tetrahydrofuran (THF). After filtering, washing with *n*-pentane, and drying of the precipitate *in vacuo*, the obtained bright yellow solid (86% isolated yield) was analyzed by means of ^{31}P and ^{1}H NMR spectroscopy in THF-d_8. In the ^{31}P NMR spectrum of **4**, the singlet resonance for the PN ligands can be found in the typical range at δ 1.9 ppm. For the phosphaureate ligand, a singlet instead of a doublet resonance is observed at δ −38.9 ppm in the ^{31}P NMR spectrum, proving successful deprotonation of the *PH* group. In addition, successful deprotonation was further indicated by the absence of the P*H* resonance in the ^{1}H NMR spectrum of **4**. Despite all our attempts, we have not been able to obtain X-ray-quality crystals suitable for a full structural elucidation. However, slow diffusion of *n*-hexane into a concentrated THF-d_8 solution of **4** yielded crystals of sufficient quality to unambiguously determine the connectivity of compound **4** in the solid state. As anticipated, the potassium salt **4** forms a one-dimensional polymeric chain in the solid state. Therein, the potassium ions are coordinated by the phosphorus atoms of the phosphaureate ligands as well as the oxygen atoms of neighboring complex molecules. Additional intra- and intermolecular interactions with arene substituents complete the coordination spheres of the potassium ions (see Figure S78 in the Supporting Information and the illustration in Scheme 4). A similar one-dimensional polymeric chain structure has been previously reported for the potassium salt **KPN**.[76]

Similarly, the reaction of **3** with KHMDS resulted in the deprotonation of the *PH* group (Scheme 4, bottom). However, even though the ^{1}H NMR spectrum of the product indicated that a quite defined material was obtained after workup, the ^{31}P NMR spectrum showed two surprisingly low field shifted singlet resonances at δ 60.8 and 10.2 ppm in addition to the typical PN ligand resonance at δ 3.3 ppm (see Figures S34 and S36 in the Supporting Information). Conducting a variable-temperature (VT) NMR spectroscopic investigation (Figures S38 and S39), we observed splitting of the initial three ^{31}P resonances at 303 K into a set of eight resonances at 243 K

https://dx.doi.org/10.1021/acs.inorgchem.0c01971
Inorg. Chem. 2020, 59, 13621−13631

(Figure S39). In addition, we noticed that the relative intensities of the ^{31}P resonances grouped at around δ 60.8 and 10.2 ppm changed from 0.83:0.17 at 303 K to roughly 0.94:0.06 at 243 K, with the sum of the PN ligand resonance intensities set to a constant relative integral of 2 (Figures S36 and S37). When the elemental analysis data were taken into account, which corroborated the formation of the desired potassium salt of **3**, the NMR spectroscopic results might suggest an equilibrium between at least two different isomers in solution. We therefore carefully hypothesize that the phosphathioureate is not only $\kappa^2(S,N)$-bound to lanthanum(III), as would be expected, but can also rearrange to the $\kappa^2(P,N)$-bound form (see Scheme 4 and Figure S36 for illustrations), since e.g. the electronegativities of the neighboring elements phosphorus and sulfur are very similar. The rather complex dynamic processes involved prevented us from isolating or crystallizing the isomers in question, and we are currently further pursuing their identification and the proper assignment of their spectroscopic features.

These findings caused us to concentrate our efforts on the defined polymeric complex **4** and its salt metathesis reactions to build heterobimetallic complexes (Scheme 5). For this we chose 1,3-bis(2,6-diisopropyphenyl)imidazol-2-ylidene (IPr)- or 1-(2,6-diisopropylphenyl)-3,3,5,5-tetramethylpyrrolidin-2-ylidene (^{Me}CAAC)-supported copper(I) and gold(I) chloride, since we assumed that these coinage-metal ions would be a good match for the rather "soft" phosphaureate P donor atom.

The use of different carbenes should also serve to demonstrate the possibility of a modular design: e.g., for fine-tuning of the electronic properties of the desired heterobimetallic systems. In addition, with regard to possible future photophysical applications, we considered the selected carbene ligands to be perfectly suited for (i) efficient steric shielding to minimize conformational flexibility as well as intermolecular interactions and (ii) a future comparison of photophysical properties with those of already reported luminescent coinage-metal carbene complexes.[80−91]

For the preparation of the heterobimetallic complexes **5** and **6** with an IPr supporting ligand at the coinage-metal ion a suspension of compound **4** and 1 equiv of either **(IPr)CuCl**[92] or **(IPr)AuCl**[93] were stirred in diethyl ether at room temperature (Scheme 5). After 10−15 min the solution of the suspension turned yellow, while the originally suspended yellow solid (starting material **4**) was replaced by a fine, colorless precipitate, indicating the formation of potassium chloride. Already at this point, reaction monitoring using ^{31}P NMR spectroscopy confirmed the full conversion to a new compound in each case. Centrifugation, filtration, and removal of the solvent *in vacuo* gave a solid which was washed with *n*-hexane or *n*-pentane and dried *in vacuo* to yield the pure product as light yellow powders in good isolated yields (80% for **5** and 76% for **6**). When the diethyl ether filtrate was allowed to rest at room temperature, reasonable amounts of crystalline material of both **5** and **6** could be obtained (*vide infra*). For the corresponding ^{Me}CAAC-supported systems **7** and **8**, with **(^{Me}CAAC)CuCl**[81] or **(^{Me}CAAC)AuCl**[94] as the starting materials (for the preparation, see the Supporting Information), similar synthesis and workup protocols were applicable. However, due to the higher solubility and the poor crystallization behavior, substantially lower yields were achieved in the case of the copper complex **7** (40%). Additionally, for complex **8** the reaction does not proceed as cleanly as for the previous examples and the impurities formed have solubilities similar to that of the anticipated complex **8**, rendering its isolation elusive as yet. Alternatively, a one-pot synthesis of heterobimetallic complexes by consecutive addition of KHMDS and **(IPr)MCl** (M = Cu, Au) to compound **2** in diethyl ether at room temperature was also found to be feasible. ^{31}P NMR spectroscopy confirmed the formation of the desired complexes **5** and **6** (see Figures S47 and S55), showing that the potassium salt **4** does not necessarily have to be isolated and at the same time emphasizing the potential of this simple reaction protocol.

Since we found salt metathesis not to be an ideal route for the isolation of complex **8**, we opted for a different approach for preparing **8**: namely, a direct protonolysis of a basic gold(I) precursor by complex **2** (Scheme 6). For this purpose, the new

Scheme 6. Alternative Route to Access Heterobimetallic Complex 8 by Reaction of 2 with (^{Me}CAAC)Au(HMDS)

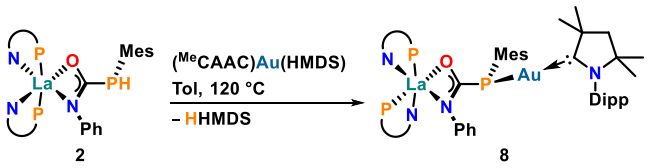

gold(I) precursor complex **(^{Me}CAAC)Au(HMDS)** containing the strongly basic bis(trimethylsilyl)amido ligand was synthesized by substitution of trimethylphosphine with ^{Me}CAAC in (Me_3P)Au(HMDS)[95] (for experimental, spectroscopic, and crystallographic details see the Experimental Section, Figures S1−S8, S70, and S77, and Tables S1 and S2 in the Supporting Information). Initially, no reaction between **2** and **(^{Me}CAAC)-Au(HMDS)** in toluene was observed when the reaction mixture was stirred at room temperature for 24 h and only traces of **8** were formed at higher temperatures of 80 °C, according to ^{31}P{^{1}H} NMR spectroscopy. However, the full consumption of starting material **2** was finally achieved through refluxing at 120 °C for 2 weeks, albeit with the formation of significant amounts of the protonated ligand **HPN**, presumably due to decomposition during the prolonged heating (see Figure S68). We attribute the slow reaction rate to the low reactivity of **(^{Me}CAAC)Au(HMDS)**, since e.g. electrophilic alkylation with benzyl bromide was not possible under conditions reported for the related literature-known complex (IPr)Au(N^iPr_2)[96] (see Figure S69). Even though the isolation of **8** was again hampered by similarly soluble impurities, the experiment still shows that in principle such heterobimetallic complexes can be also obtained by the reaction of **2** with transition-metal amide precursors.

The new heterobimetallic complexes were analyzed by means of multinuclear NMR spectroscopy in C_6D_6. Although we were unable to obtain pure material of complex **8**, the respective distinctive NMR resonances can be confidently assigned, especially in the ^{13}C{^{1}H} and ^{31}P NMR spectra (see the Experimental Section and Figures S65−S67 in the Supporting Information). Despite the complexity of the target compounds **5**−**8**, their ^{1}H NMR spectra were found to contain astonishingly sharp and well separated resonances, especially in the aromatic region (see Figures S40, S48, S56, and S65 in the Supporting Information), pointing to a high conformational rigidity of the heterobimetallic systems in solution. In addition, the fact that only one set of resonances of the complexes **5**−**8** is present in each ^{1}H NMR spectrum suggests the selective formation of one particular isomer, respectively. Apart from the

https://dx.doi.org/10.1021/acs.inorgchem.0c01971
Inorg. Chem. 2020, 59, 13621−13631

Table 1. Selected $^{13}C\{^1H\}$ and ^{31}P NMR Data of Heterobimetallic Complexes 5−8 in C_6D_6 at 303 K, with Chemical Shifts δ in ppm

	$^{13}C\{^1H\}$ NMR		^{31}P NMR	
complex	$C_{carbene}$	$C_{phosphaureate}$	PN^-	$P_{phosphaureate}$
5	182.9 (d, $^2J_{CP}$ = 44 Hz)	201.5 (br s)	3.7 (s)	−65.0 (s)
6	197.4 (d, $^2J_{CP}$ = 66 Hz)	201.6 (br s)	4.0 (s)	−42.0 (s)
7	251.4 (d, $^2J_{CP}$ = 42 Hz)	201.3 (d, $^1J_{CP}$ = 46 Hz)	3.7 (s)	−63.7 (s)
8	258.4 (d, $^2J_{CP}$ = 62 Hz)	202.2 (d, $^1J_{CP}$ = 48 Hz)	3.8 (s)	−38.2 (s)

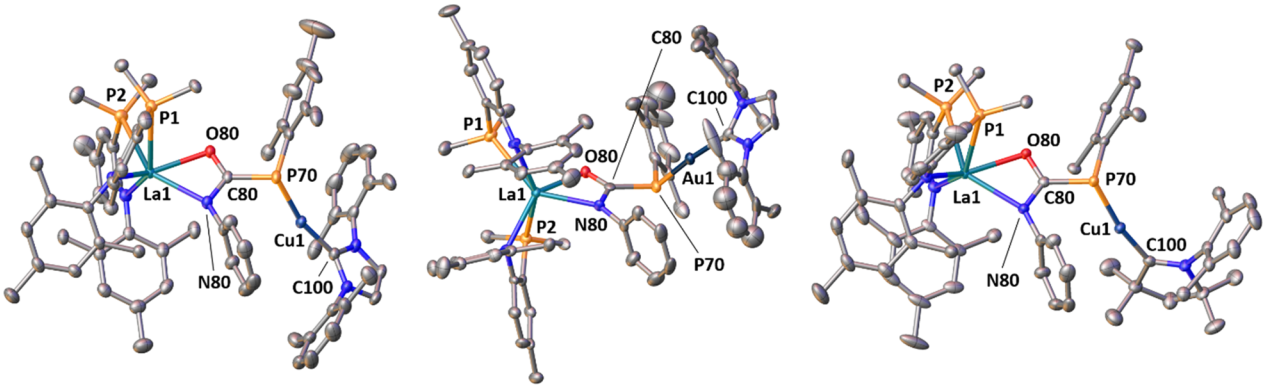

Figure 3. Thermal ellipsoid plots of **5**−**7** (from left to right). Thermal ellipsoids are shown at a probability level of 30%. Hydrogen atoms have been omitted and ^{i}Pr groups truncated for clarity.

appearance of a new set of carbene ligand resonances in the ^1H NMR spectra, the $^{13}C\{^1H\}$ NMR data obtained for **5**−**8** most clearly show the successful coordination of the different coinage-metal carbene fragments to the phosphaureate ligand (Table 1, left).

For the IPr systems **5** and **6** chemical shifts between δ 180 and 200 ppm for the $C_{carbene}$ resonance were recorded, while for the ^{Me}CAAC analogs **7** and **8** these resonances lay at lower fields of δ 250−260 ppm, as is typical of CAACs in comparison to NHCs.[97] Due to the higher electronegativity of gold(I),[98] the $C_{carbene}$ resonances of the gold(I) systems **6** and **8** are shifted to lower fields compared to the respective copper(I) analogues **5** and **7**. More importantly, all $C_{carbene}$ resonances show a doublet splitting due to characteristic $^2J_{CP}$ coupling to the $P_{phosphaureate}$ atom, thereby confirming coordination of the phosphaureate ligand via the P donor atom. The $^2J_{CP}$ coupling constants for the gold(I) complexes **6** and **8** of 60−70 Hz are considerably larger than for the copper(I) compounds **5** and **7** (40−45 Hz), possibly indicating a stronger binding of the gold(I) carbene fragment to phosphorus. Overall, the determined $^2J_{CP}$ values are smaller than those for the reference complexes $[(IPr)Au(P^tBu_3)][BF_4]$[99] ($^2J_{CP}$ = 112 Hz) and $[(IPr)Cu(P^tBu_3)][BF_4]$[100] ($^2J_{CP}$ = 61 Hz), which is in line with an inferior electron-donating ability of the bridging phosphaureate ligand in **5**−**8** in comparison to tertiary phosphines. Interestingly, the shift of the $C_{phosphaureate}$ resonance (δ ∼201−202 ppm) is essentially unaffected by the choice of coinage-metal ion or carbene supporting ligand, although it is noteworthy that only for the ^{Me}CAAC systems **7** and **8** doublet splittings of $^1J_{CP}$ = 46 and 48 Hz can be determined, respectively.

A ^{31}P NMR spectroscopic study of complexes **5**−**8** revealed that binding of copper(I) or gold(I) carbene to the phosphaureate ligand can also be easily followed by the shift of the $P_{phosphaureate}$ resonance (Table 1, right). In comparison to copper(I) complexes **5** and **7** (δ −63 to −65 ppm) resonances at lower fields of δ −38 to −42 ppm were recorded in the case of gold(I) complexes **6** and **8**, as would be expected for more electronegative gold(I). The type of carbene influences the ^{31}P shift of the phosphaureate bridging ligand in terms of slightly low field shifted resonances for the ^{Me}CAAC systems **7** and **8**, presumably due to the superior π-acceptor properties of CAACs versus NHCs.[81,87,101] The PN ligand resonances behave nearly the same for the whole series **5**−**8** and are shifted only slightly to higher fields by about 2 ppm in comparison to complex **2**.

For the three heterobimetallic complexes **5**−**7** structural proof was finally obtained by X-ray crystallography (Figure 3). Suitable single crystals for diffraction analysis of **5** and **6** were obtained by storing concentrated diethyl ether solutions of the corresponding complexes at room temperature (*vide supra*). In the case of **7**, slow evaporation of a concentrated toluene solution at room temperature yielded single crystals of suitable quality. Unfortunately, we have not been able to obtain X-ray-quality crystals for complex **8** by any methods investigated as yet.

All three compounds **5**−**7** crystallize in the monoclinic space group $P2_1/c$ with one molecule in the asymmetric unit and no solvent molecules in the lattice. In each case the unprecedented $\mu,\kappa^2(O,N):\kappa^1(P)$ binding mode of the phosphaureate bridging ligand, which was already inferred from the NMR spectroscopic features, can be confirmed. Interestingly, the coordination of the coinage-metal carbene fragments to the phosphaureate ligand induced an isomerization in the coordination sphere of La1: i.e., the relative arrangement of the ^{i}Pr$_2$-phosphanyl groups of the PN supporting ligands changed from *trans* in **2** (and **4**) to *cis* in **5**−**7**, exhibiting P1−La1−P2 angles between 84.79(4) and 88.09(2)°. Apart from the La1−N80 distances, which are about 0.1 Å shorter, all other bond metrics of the phosphaureate bridging ligand in **5**−**7** are found to be essentially the same as in compound **2** (see Table S2 in the Supporting Information). For the coinage-

https://dx.doi.org/10.1021/acs.inorgchem.0c01971
Inorg. Chem. 2020, 59, 13621−13631

metal carbene fragments bound to P70 merely subtle structural differences can be asserted, which most likely result from packing effects. The P70−Cu1 bond lengths in **5** and **7** (both 2.2043(7) Å) and the P70−Au1 distance in **6** (2.314(2) Å) fall into the range of the reference complexes [(IPr)M(P^tBu_3)][BF_4] (M = Cu, Au).[99,100] The same applies for the Cu1/Au1−C100 distances,[99,100] whereas the P70−Cu1/Au1−C100 angles between 164.57(7) and 169.57(8)° in **5**−**7** clearly deviate from linearity, most likely due to steric repulsion between the carbene ligand and the phosphaureate phenyl as well as mesityl group. The C80−P70−Cu1/Au1 angle in **7** (114.16(9)°) is somewhat larger than in **5** (111.03(7)°) or **6** (110.1(2)°), which might reflect a better ability of the unsymmetrical Cu(^{Me}CAAC) fragment to bend in one (sterically preferred) direction. For more details on the crystallographic data of **5**−**7** see Tables S1 and S2 in the Supporting Information.

In this context, one interesting stereochemical property of this first set of examples of a phosphaureate bridging ligand is worth mentioning. Since the phosphaureate ligand is locked in position by its $\kappa^2(O,N)$ binding mode to lanthanum, the coinage-metal carbene fragment bound to P70 can lie either in the hemisphere above or beneath the O80−N80−P70 plane, when one looks along the La1−C80−P70 trajectory shown in Figure 4. This is expressed by positive N80−C80−P70−Cu1

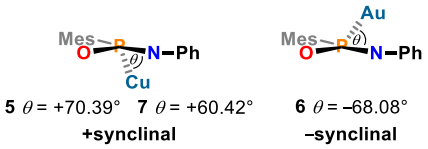

Figure 4. Views along the La1−C80−P70 trajectory in **5** and **7** (left) or **6** (right), respectively. The representations of **5**−**7** are simplified for clarity (i.e., no La$(PN)_2$ fragment or carbene ligand shown), and N80−C80−P70−Cu1/Au1 dihedral angles θ are given.

dihedral angles θ of +70.39 and +60.42° in **5** and **7**, respectively, in comparison to a negative N80−C80−P70−Au1 dihedral angle θ of −68.08° in the case of **6**. Even though already at this point it appears that there are different preferences for copper(I) (+synclinal) and gold(I) (−synclinal), a larger number of comparable examples is required to delineate conclusive parameters on how the stereochemical outcome in these heterobimetallic complexes is governed.

CONCLUSION

In conclusion, we have presented an attractive, straightforward route for the synthesis of a series of unprecedented heterobimetallic lanthanum−copper(I) and lanthanum−gold(I) complexes. Capitalizing on the insertion reactivity of the La−P primary phosphide bond in **1** toward phenyl iso(thio)cyanate, we were able to isolate **2** and **3** as rare examples of phospha(thio)ureate complexes of lanthanum(III). The retention of the P*H* proton was key to further functionalization: i.e., deprotonation and subsequent salt metathesis in the case of **2** to yield polymeric potassium salt **4** and furnish the new heterobimetallic complexes **5**−**8**, containing the first example of a phosphaureate bridging ligand with an unprecedented $\kappa^2(O,N):\kappa^1(P)$ binding mode. Additionally, compound **8** can be obtained by protonolysis of (**^{Me}CAAC**)-**Au(HMDS)** with complex **2**. For **5** and **6**, we found that the two-step reaction sequence with intermediary isolation of **4** can be replaced by a one-pot reaction protocol, further emphasizing the simplicity with which such heterobimetallic systems can be constructed. All target compounds were analyzed in detail by NMR spectroscopic techniques and by X-ray diffraction analysis (except for complex **8**). Despite the high complexity of **5**−**8**, NMR spectroscopic investigations pointed to a high conformational rigidity of each compound in solution. X-ray diffraction studies of **5**−**7** revealed two stereochemically distinguishable coordination possibilities at $P_{phosphaureate}$ for the coinage-metal ion. In the future, our modular approach, as exemplified in this work by insertion of different organic substrates into the La−P primary phosphide bond as well as a variation of carbene supporting ligand and coinage-metal ion, should give access to a wide range of carefully designed heterobimetallic lanthanide(III)−coinage-metal complexes with intriguing properties for photochemistry and catalysis.

ASSOCIATED CONTENT

Supporting Information

The Supporting Information is available free of charge at https://pubs.acs.org/doi/10.1021/acs.inorgchem.0c01971.

Experimental section, all NMR and IR spectroscopy data, crystallographic details on the complexes (**^{Me}CAAC)Au(HMDS)**, **2**, **3**, and **5**−**7**, the molecular structure of (**^{Me}CAAC)Au(HMDS)**, and the connectivity found in polymeric **4** (PDF)

Accession Codes

CCDC 2012278−2012283 contain the supplementary crystallographic data for this paper. These data can be obtained free of charge via www.ccdc.cam.ac.uk/data_request/cif, or by emailing data_request@ccdc.cam.ac.uk, or by contacting The Cambridge Crystallographic Data Centre, 12 Union Road, Cambridge CB2 1EZ, UK; fax: +44 1223 336033.

AUTHOR INFORMATION

Corresponding Author

Stephan Hohloch − *University of Innsbruck, Faculty of Chemistry and Pharmacy, Institute of General, Inorganic and Theoretical Chemistry, 6020 Innsbruck, Austria;* orcid.org/0000-0002-5353-0801; Email: Stephan.Hohloch@uibk.ac.at

Authors

Fabian A. Watt − *Paderborn University, Faculty of Science, Department of Chemistry, 33098 Paderborn, Germany;* orcid.org/0000-0002-2213-0864

Nicole Dickmann − *Paderborn University, Faculty of Science, Department of Chemistry, 33098 Paderborn, Germany*

Roland Schoch − *Paderborn University, Faculty of Science, Department of Chemistry, 33098 Paderborn, Germany;* orcid.org/0000-0003-2061-7289

Complete contact information is available at: https://pubs.acs.org/10.1021/acs.inorgchem.0c01971

Author Contributions

The project was designed by S.H. and F.A.W. Experimental work was carried out by F.A.W. and N.D. NMR and IR spectra were recorded by F.A.W. and N.D. X-ray structure analyses were performed by R.S. and S.H. The manuscript was written by F.A.W. and S.H. and proofread by all authors. All authors have given approval to the final version of the manuscript.

https://dx.doi.org/10.1021/acs.inorgchem.0c01971
Inorg. Chem. 2020, 59, 13621−13631

Notes

The authors declare no competing financial interest.

■ ACKNOWLEDGMENTS

We are grateful to the Daimler and Benz Foundation, the Fonds der Chemischen Industrie, the Young Academy of the North-Rhine-Westphalian Academy of Sciences, Humanities and the Arts, Paderborn University, and the University of Innsbruck for financial support. Additionally, we thank Prof. Dr. Matthias Bauer for continuous support and fruitful discussions. Dr. Hans Egold from the NMR facility of the Paderborn University is kindly acknowledged for helpful discussions. Christiane Gloger and Maria Busse are kindly acknowledged for conducting elemental analyses.

■ REFERENCES

(1) Liddle, S. T. International Year of the Periodic Table: Lanthanide and Actinide Chemistry. *Angew. Chem., Int. Ed.* **2019**, *58*, 5140−5141.
(2) Martinez-Gomez, N. C.; Vu, H. N.; Skovran, E. Lanthanide Chemistry: From Coordination in Chemical Complexes Shaping Our Technology to Coordination in Enzymes Shaping Bacterial Metabolism. *Inorg. Chem.* **2016**, *55*, 10083−10089.
(3) Day, B. M.; Guo, F.-S.; Layfield, R. A. Cyclopentadienyl Ligands in Lanthanide Single-Molecule Magnets: One Ring To Rule Them All? *Acc. Chem. Res.* **2018**, *51*, 1880−1889.
(4) Guo, F.-S.; Day, B. M.; Chen, Y.-C.; Tong, M.-L.; Mansikkamäki, A.; Layfield, R. A. Magnetic hysteresis up to 80 K in a dysprosium metallocene single-molecule magnet. *Science* **2018**, *362*, 1400−1403.
(5) Goodwin, C. A. P.; Ortu, F.; Reta, D.; Chilton, N. F.; Mills, D. P. Molecular magnetic hysteresis at 60 K in dysprosocenium. *Nature* **2017**, *548*, 439−442.
(6) Randall McClain, K.; Gould, C. A.; Chakarawet, K.; Teat, S. J.; Groshens, T. J.; Long, J. R.; Harvey, B. G. High-temperature magnetic blocking and magneto-structural correlations in a series of dysprosium(iii) metallocenium single-molecule magnets. *Chem. Sci.* **2018**, *9*, 8492−8503.
(7) Guo, F.-S.; Day, B. M.; Chen, Y.-C.; Tong, M.-L.; Mansikkamäki, A.; Layfield, R. A. A Dysprosium Metallocene Single-Molecule Magnet Functioning at the Axial Limit. *Angew. Chem., Int. Ed.* **2017**, *56*, 11445−11449.
(8) Gould, C. A.; McClain, K. R.; Yu, J. M.; Groshens, T. J.; Furche, F.; Harvey, B. G.; Long, J. R. Synthesis and Magnetism of Neutral, Linear Metallocene Complexes of Terbium(II) and Dysprosium(II). *J. Am. Chem. Soc.* **2019**, *141*, 12967−12973.
(9) Gould, C. A.; Darago, L. E.; Gonzalez, M. I.; Demir, S.; Long, J. R. A Trinuclear Radical-Bridged Lanthanide Single-Molecule Magnet. *Angew. Chem., Int. Ed.* **2017**, *56*, 10103−10107.
(10) Demir, S.; Zadrozny, J. M.; Nippe, M.; Long, J. R. Exchange coupling and magnetic blocking in bipyrimidyl radical-bridged dilanthanide complexes. *J. Am. Chem. Soc.* **2012**, *134*, 18546−18549.
(11) Demir, S.; Gonzalez, M. I.; Darago, L. E.; Evans, W. J.; Long, J. R. Giant coercivity and high magnetic blocking temperatures for N_2^{3-} radical-bridged dilanthanide complexes upon ligand dissociation. *Nat. Commun.* **2017**, *8*, 2144.
(12) Bünzli, J.-C. G. Lanthanide luminescence for biomedical analyses and imaging. *Chem. Rev.* **2010**, *110*, 2729−2755.
(13) Mohamadi, A.; Miller, L. W. Brightly Luminescent and Kinetically Inert Lanthanide Bioprobes Based on Linear and Preorganized Chelators. *Bioconjugate Chem.* **2016**, *27*, 2540−2548.
(14) Oukhatar, F.; Eliseeva, S. V.; Bonnet, C. S.; Placidi, M.; Logothetis, N. K.; Petoud, S.; Angelovski, G.; Tóth, É. Toward MRI and Optical Detection of Zwitterionic Neurotransmitters: Near-Infrared Luminescent and Magnetic Properties of Macrocyclic Lanthanide(III) Complexes Appended with a Crown Ether and a Benzophenone Chromophore. *Inorg. Chem.* **2019**, *58*, 13619−13630.
(15) Wu, S.-Y.; Guo, X.-Q.; Zhou, L.-P.; Sun, Q.-F. Fine-Tuned Visible and Near-Infrared Luminescence on Self-Assembled Lanthanide-Organic Tetrahedral Cages with Triazole-Based Chelates. *Inorg. Chem.* **2019**, *58*, 7091−7098.
(16) Barger, C. J.; Motta, A.; Weidner, V. L.; Lohr, T. L.; Marks, T. J. $La[N(SiMe_3)_2]_3$-Catalyzed Ester Reductions with Pinacolborane: Scope and Mechanism of Ester Cleavage. *ACS Catal.* **2019**, *9*, 9015−9024.
(17) Basiouny, M. M. I.; Dollard, D. A.; Schmidt, J. A. R. Regioselective Single and Double Hydrophosphination and Hydrophosphinylation of Unactivated Alkynes. *ACS Catal.* **2019**, *9*, 7143−7153.
(18) Chen, W.; Song, H.; Li, J.; Cui, C. Catalytic Selective Dihydrosilylation of Internal Alkynes Enabled by Rare-Earth Ate Complex. *Angew. Chem., Int. Ed.* **2020**, *59*, 2365−2369.
(19) Gurina, G. A.; Kissel, A. A.; Lyubov, D. M.; Luconi, L.; Rossin, A.; Tuci, G.; Cherkasov, A. V.; Lyssenko, K. A.; Shavyrin, A. S.; Ob'edkov, A. M.; Giambastiani, G.; Trifonov, A. A. Bis(alkyl) scandium and yttrium complexes coordinated by an amidopyridinate ligand: synthesis, characterization and catalytic performance in isoprene polymerization, hydroelementation and carbon dioxide hydrosilylation. *Dalton Trans.* **2020**, *49*, 638−650.
(20) Kazeminejad, N.; Munzel, D.; Gamer, M. T.; Roesky, P. W. Bis(amidinate) ligands in early lanthanide chemistry − synthesis, structures, and hydroamination catalysis. *Chem. Commun.* **2017**, *53*, 1060−1063.
(21) Qiao, Y.; Schelter, E. J. Lanthanide Photocatalysis. *Acc. Chem. Res.* **2018**, *51*, 2926−2936.
(22) Qiao, Y.; Yang, Q.; Schelter, E. J. Photoinduced Miyaura Borylation by a Rare-Earth-Metal Photoreductant: The Hexachlorocerate(III) Anion. *Angew. Chem., Int. Ed.* **2018**, *57*, 10999−11003.
(23) Edelmann, F. T. Lanthanide amidinates and guanidinates in catalysis and materials science: a continuing success story. *Chem. Soc. Rev.* **2012**, *41*, 7657−7672.
(24) Gu, X.; Zhang, L.; Zhu, X.; Wang, S.; Zhou, S.; Wei, Y.; Zhang, G.; Mu, X.; Huang, Z.; Hong, D.; Zhang, F. Synthesis of Bis(NHC)-Based CNC-Pincer Rare-Earth-Metal Amido Complexes and Their Application for the Hydrophosphination of Heterocumulenes. *Organometallics* **2015**, *34*, 4553−4559.
(25) Kissel, A. A.; Mahrova, T. V.; Lyubov, D. M.; Cherkasov, A. V.; Fukin, G. K.; Trifonov, A. A.; Del Rosal, I.; Maron, L. Metallacyclic yttrium alkyl and hydrido complexes: synthesis, structures and catalytic activity in intermolecular olefin hydrophosphination and hydroamination. *Dalton Trans.* **2015**, *44*, 12137−12148.
(26) Basalov, I. V.; Yurova, O. S.; Cherkasov, A. V.; Fukin, G. K.; Trifonov, A. A. Amido Ln(II) Complexes Coordinated by Bi- and Tridentate Amidinate Ligands: Nonconventional Coordination Modes of Amidinate Ligands and Catalytic Activity in Intermolecular Hydrophosphination of Styrenes and Tolane. *Inorg. Chem.* **2016**, *55*, 1236−1244.
(27) Basiouny, M. M. I.; Schmidt, J. A. R. Lanthanum-Catalyzed Double Hydrophosphinylation of Nitriles. *Organometallics* **2017**, *36*, 721−729.
(28) Behrle, A. C.; Schmidt, J. A. R. Insertion Reactions and Catalytic Hydrophosphination of Heterocumulenes using α-Metalated *N*,*N*-Dimethylbenzylamine Rare-Earth-Metal Complexes. *Organometallics* **2013**, *32*, 1141−1149.
(29) Rina, Y. A.; Schmidt, J. A. R. Lanthanum-Catalyzed Regioselective Anti-Markovnikov Hydrophosphinylation of Styrenes. *Organometallics* **2019**, *38*, 4261−4270.
(30) Trifonov, A. A.; Basalov, I. V.; Kissel, A. A. Use of organolanthanides in the catalytic intermolecular hydrophosphination and hydroamination of multiple C−C bonds. *Dalton Trans.* **2016**, *45*, 19172−19193.
(31) Zhang, W.-X.; Nishiura, M.; Mashiko, T.; Hou, Z. Half-sandwich *o*-*N*,*N*-dimethylaminobenzyl complexes over the full size range of group 3 and lanthanide metals. synthesis, structural

https://dx.doi.org/10.1021/acs.inorgchem.0c01971
Inorg. Chem. 2020, 59, 13621−13631

characterization, and catalysis of phosphine P−H bond addition to carbodiimides. *Chem. - Eur. J.* **2008**, *14*, 2167−2179.
(32) Yin, H.; Carroll, P. J.; Manor, B. C.; Anna, J. M.; Schelter, E. J. Cerium Photosensitizers: Structure-Function Relationships and Applications in Photocatalytic Aryl Coupling Reactions. *J. Am. Chem. Soc.* **2016**, *138*, 5984−5993.
(33) Qiao, Y.; Cheisson, T.; Manor, B. C.; Carroll, P. J.; Schelter, E. J. A strategy to improve the performance of cerium(iii) photocatalysts. *Chem. Commun.* **2019**, *55*, 4067−4070.
(34) Manzur, J.; Poblete, C.; Morales, J.; de Santana, R. C.; Queiroz Maia, L. J.; Vega, A.; Fuentealba, P.; Spodine, E. Enhancement of Terbium(III)-Centered Luminescence by Tuning the Triplet Energy Level of Substituted Pyridylamino-4-R-Phenoxo Tripodal Ligands. *Inorg. Chem.* **2020**, *59*, 5447−5455.
(35) Rinehart, J. D.; Long, J. R. Exploiting single-ion anisotropy in the design of f-element single-molecule magnets. *Chem. Sci.* **2011**, *2*, 2078.
(36) Bag, P.; Goura, J.; Mereacre, V.; Novitchi, G.; Powell, A. K.; Chandrasekhar, V. Synthesis, magnetism and Mössbauer studies of tetranuclear heterometallic $\{Fe^{III}_2Ln_2\}$(Ln = Gd, Dy, Tb) complexes: evidence of slow relaxation of magnetization in the terbium analogue. *Dalton Trans.* **2014**, *43*, 16366−16376.
(37) Burns, C. P.; Yang, X.; Wofford, J. D.; Bhuvanesh, N. S.; Hall, M. B.; Nippe, M. Structure and Magnetization Dynamics of Dy−Fe and Dy−Ru Bonded Complexes. *Angew. Chem., Int. Ed.* **2018**, *57*, 8144−8148.
(38) Rigamonti, L.; Nava, A.; Boulon, M.-E.; Luzon, J.; Sessoli, R.; Cornia, A. Experimental and Theoretical Studies on the Magnetic Anisotropy in Lanthanide(III)-Centered Fe_3Ln Propellers. *Chem. - Eur. J.* **2015**, *21*, 12171−12180.
(39) Singh, N.; Das Gupta, S.; Butcher, R. J.; Christou, G. Synthesis and magnetochemistry of heterometallic triangular $Fe^{III}_2Ln^{III}$ (Ln = La, Gd, Tb, Dy, and Ho) and $Fe^{III}_2Y^{III}$ complexes. *Dalton Trans.* **2017**, *46*, 7897−7903.
(40) Wang, H.-S.; Long, Q.-Q.; Hu, Z.-B.; Yue, L.; Yang, F.-J.; Yin, C.-L.; Pan, Z.-Q.; Zhang, Y.-Q.; Song, Y. Synthesis, crystal structures and magnetic properties of a series of chair-like heterometallic $[Fe_4Ln_2]$ (Ln = Gd^{III}, Dy^{III}, Ho^{III}, and Er^{III}) complexes with mixed organic ligands. *Dalton Trans.* **2019**, *48*, 13472−13482.
(41) Stoian, S. A.; Paraschiv, C.; Kiritsakas, N.; Lloret, F.; Münck, E.; Bominaar, E. L.; Andruh, M. Mössbauer, electron paramagnetic resonance, and magnetic susceptibility studies on members of a new family of cyano-bridged 3d-4f complexes. Demonstration of anisotropic exchange in a Fe−Gd complex. *Inorg. Chem.* **2010**, *49*, 3387−3401.
(42) Qiu, J.-Z.; Wang, L.-F.; Chen, Y.-C.; Zhang, Z.-M.; Li, Q.-W.; Tong, M.-L. Magnetocaloric Properties of Heterometallic 3d−Gd Complexes Based on the $[Gd(oda)_3]^{3-}$ Metalloligand. *Chem. - Eur. J.* **2016**, *22*, 802−808.
(43) Burns, C. P.; Yang, X.; Sung, S.; Wofford, J. D.; Bhuvanesh, N. S.; Hall, M. B.; Nippe, M. Towards understanding of lanthanide-transition metal bonding: investigations of the first Ce−Fe bonded complex. *Chem. Commun.* **2018**, *54*, 10893−10896.
(44) Ahmed, N.; Das, C.; Vaidya, S.; Langley, S. K.; Murray, K. S.; Shanmugam, M. Nickel(II)−lanthanide(III) magnetic exchange coupling influencing single-molecule magnetic features in $\{Ni_2Ln_2\}$ complexes. *Chem. - Eur. J.* **2014**, *20*, 14235−14239.
(45) Ahmed, N.; Das, C.; Vaidya, S.; Srivastava, A. K.; Langley, S. K.; Murray, K. S.; Shanmugam, M. Probing the magnetic and magneto-thermal properties of M(II)−Ln(III) complexes (where M(II) = Ni or Zn; Ln(III) = La or Pr or Gd). *Dalton Trans.* **2014**, *43*, 17375−17384.
(46) Upadhyay, A.; Das, C.; Langley, S. K.; Murray, K. S.; Srivastava, A. K.; Shanmugam, M. Heteronuclear Ni(ii)−Ln(iii) (Ln = La, Pr, Tb, Dy) complexes: synthesis and single-molecule magnet behaviour. *Dalton Trans.* **2016**, *45*, 3616−3626.
(47) Vieru, V.; Pasatoiu, T. D.; Ungur, L.; Suturina, E.; Madalan, A. M.; Duhayon, C.; Sutter, J.-P.; Andruh, M.; Chibotaru, L. F. Synthesis, Crystal Structures, Magnetic Properties, and Theoretical Investigation of a New Series of Ni^{II}−Ln^{III}−W^{V} Heterotrimetallics: Understanding the SMM Behavior of Mixed Polynuclear Complexes. *Inorg. Chem.* **2016**, *55*, 12158−12171.
(48) Long, J.; Rouquette, J.; Thibaud, J.-M.; Ferreira, R. A. S.; Carlos, L. D.; Donnadieu, B.; Vieru, V.; Chibotaru, L. F.; Konczewicz, L.; Haines, J.; Guari, Y.; Larionova, J. A high-temperature molecular ferroelectric Zn/Dy complex exhibiting single-ion-magnet behavior and lanthanide luminescence. *Angew. Chem., Int. Ed.* **2015**, *54*, 2236−2240.
(49) Upadhyay, A.; Singh, S. K.; Das, C.; Mondol, R.; Langley, S. K.; Murray, K. S.; Rajaraman, G.; Shanmugam, M. Enhancing the effective energy barrier of a Dy(III) SMM using a bridged diamagnetic Zn(II) ion. *Chem. Commun.* **2014**, *50*, 8838−8841.
(50) Chen, F.-F.; Bian, Z.-Q.; Liu, Z.-W.; Nie, D.-B.; Chen, Z.-Q.; Huang, C.-H. Highly efficient sensitized red emission from europium (III) in Ir−Eu bimetallic complexes by ^{3}MLCT energy transfer. *Inorg. Chem.* **2008**, *47*, 2507−2513.
(51) Shavaleev, N. M.; Accorsi, G.; Virgili, D.; Bell, Z. R.; Lazarides, T.; Calogero, G.; Armaroli, N.; Ward, M. D. Syntheses and crystal structures of dinuclear complexes containing d-block and f-block luminophores. Sensitization of NIR luminescence from Yb(III), Nd(III), and Er(III) centers by energy transfer from Re(I)- and Pt(II)-bipyrimidine metal centers. *Inorg. Chem.* **2005**, *44*, 61−72.
(52) Shavaleev, N. M.; Moorcraft, L. P.; Pope, S. J. A.; Bell, Z. R.; Faulkner, S.; Ward, M. D. Sensitised near-infrared emission from lanthanides using a covalently-attached Pt(II) fragment as an antenna group. *Chem. Commun.* **2003**, 1134−1135.
(53) Shavaleev, N. M.; Moorcraft, L. P.; Pope, S. J. A.; Bell, Z. R.; Faulkner, S.; Ward, M. D. Sensitized near-infrared emission from complexes of Yb^{III}, Nd^{III} and Er^{III} by energy-transfer from covalently attached Pt^{II}-based antenna units. *Chem. - Eur. J.* **2003**, *9*, 5283−5291.
(54) Zakrzewski, J. J.; Sieklucka, B.; Chorazy, S. Europium(III) Photoluminescence Governed by d^8-d^{10} Heterometallophilic Interactions in Trimetallic Cyanido-Bridged Coordination Frameworks. *Inorg. Chem.* **2020**, *59*, 1393−1404.
(55) Wen, H.-R.; Hu, J.-J.; Yang, K.; Zhang, J.-L.; Liu, S.-J.; Liao, J.-S.; Liu, C.-M. Family of Chiral Zn^{II}−Ln^{III} (Ln = Dy and Tb) Heterometallic Complexes Derived from the Amine-Phenol Ligand Showing Multifunctional Properties. *Inorg. Chem.* **2020**, *59*, 2811−2824.
(56) Li, X.-L.; Zhang, K.-J.; Li, J.-J.; Cheng, X.-X.; Chen, Z.-N. Dual Luminescent Dinuclear Gold(I) Complexes of Terpyridyl-Functionalized Alkyne Ligands and Their Efficient Sensitization of Eu^{III} and Yb^{III} Luminescence. *Eur. J. Inorg. Chem.* **2010**, *2010*, 3449−3457.
(57) Xu, H.-B.; Zhang, L.-Y.; Ni, J.; Chao, H.-Y.; Chen, Z.-N. Conformation changes and luminescent properties of Au−Ln (Ln = Nd, Eu, Er, Yb) arrays with 5-ethynyl-2,2'-bipyridine. *Inorg. Chem.* **2008**, *47*, 10744−10752.
(58) Klink, S. I.; Keizer, H.; van Veggel, F. C. J. M. Transition Metal Complexes as Photosensitizers for Near-Infrared Lanthanide Luminescence. *Angew. Chem., Int. Ed.* **2000**, *39*, 4319−4321.
(59) Chen, F.-F.; Chen, Z.-Q.; Bian, Z.-Q.; Huang, C.-H. Sensitized luminescence from lanthanides in d−f bimetallic complexes. *Coord. Chem. Rev.* **2010**, *254*, 991−1010.
(60) Sakamoto, M.; Manseki, K.; Okawa, H. d−f Heteronuclear complexes: synthesis, structures and physicochemical aspects. *Coord. Coord. Chem. Rev.* **2001**, *219−221*, 379−414.
(61) Yi, W.; Zhang, J.; Hong, L.; Chen, Z.; Zhou, X. Insertion of Isocyanate and Isothiocyanate into the Ln−P σ-Bond of Organolanthanide Phosphides. *Organometallics* **2011**, *30*, 5809−5814.
(62) Garner, M. E.; Parker, B. F.; Hohloch, S.; Bergman, R. G.; Arnold, J. Thorium Metallacycle Facilitates Catalytic Alkyne Hydrophosphination. *J. Am. Chem. Soc.* **2017**, *139*, 12935−12938.
(63) Lindenberg, F.; Sieler, J.; Hey-Hawkins, E. FORMATION OF NOVEL P- AND As-FUNCTIONALIZED LIGANDS BY INSERTION REACTIONS INTO THE Zr−E BOND OF $(\eta^5$-$C_5H_4R)_2ZrCl\{E(SiMe_3)_2\}$ (R = Me, E = P, As; R = H, E = P). *Polyhedron* **1996**, *15*, 1459−1471.

https://dx.doi.org/10.1021/acs.inorgchem.0c01971
Inorg. Chem. 2020, 59, 13621−13631

(64) Segerer, U.; Sieler, J.; Hey-Hawkins, E. Formation of Novel P-Functionalized Ligands by Insertion Reactions of RNCX (R = Ph, X = O, S; R = Pr^i, X = O) into the Zr−P Bond of $[Cp^\circ_2ZrCl(PHCy)]$ (Cp° = η^5-C_5EtMe_4, Cy = Cyclohexyl) and $[Cp^\iota_2ZrCl\{PH(TRIP)\}]$ (Cp^ι = η^5 -C_5MeH_4, TRIP = 2,4,6-$Pr^i_3C_6H_2$). *Organometallics* **2000**, *19*, 2445−2449.
(65) Hou, Z.; Stephan, D. W. Generation and Reactivity of the First Mononuclear Early Metal Phosphinidene Complex, Cp^*_2Zr = $P(C_6H_2Me_3$-2,4,6). *J. Am. Chem. Soc.* **1992**, *114*, 10088−10089.
(66) Hou, Z.; Breen, T. L.; Stephan, D. W. Formation and Reactivity of the Early Metal Phosphides and Phosphinidenes Cp^*_2Zr = PR, $Cp^*_2Zr(PR)_2$, and $Cp^*_2Zr(PR)_3$. *Organometallics* **1993**, *12*, 3158−3167.
(67) Vilanova, S. P.; Tarlton, M. L.; Barnes, C. L.; Walensky, J. R. Double insertion of benzophenone into thorium−phosphorus bonds. *J. Organomet. Chem.* **2018**, *857*, 159−163.
(68) Vilanova, S. P.; Del Rosal, I.; Tarlton, M. L.; Maron, L.; Walensky, J. R. Functionalization of Carbon Monoxide and *tert*-Butyl Nitrile by Intramolecular Proton Transfer in a Bis(Phosphido) Thorium Complex. *Angew. Chem., Int. Ed.* **2018**, *57*, 16748−16753.
(69) Behrle, A. C.; Walensky, J. R. Insertion of ^{t}BuNC into thorium−phosphorus and thorium−arsenic bonds: phosphaazaallene and arsaazaallene moieties in f element chemistry. *Dalton Trans.* **2016**, *45*, 10042−10049.
(70) Zhang, C.; Wang, Y.; Hou, G.; Ding, W.; Zi, G.; Walter, M. D. Experimental and computational studies on a three-membered diphosphido thorium metallaheterocycle $[\eta^5$-1,3-$(Me_3C)_2C_5H_3]_2$Th-$[\eta^2$-$P_2(2,4,6$-$^iPr_3C_6H_2)_2]$. *Dalton Trans.* **2019**, *48*, 6921−6930.
(71) Tarlton, M. L.; Del Rosal, I.; Vilanova, S. P.; Kelley, S. P.; Maron, L.; Walensky, J. R. Comparative Insertion Reactivity of CO, CO_2, ^{t}BuCN, and ^{t}BuNC into Thorium− and Uranium−Phosphorus Bonds. *Organometallics* **2020**, *39*, 2152−2161.
(72) Rungthanaphatsophon, P.; Fajen, O. J.; Kelley, S. P.; Walensky, J. R. Thorium(IV) and Uranium(IV) Phosphaazaallenes. *Inorganics* **2019**, *7*, 105.
(73) Ward, R. J.; Rungthanaphatsophon, P.; Rosal, I. d.; Kelley, S. P.; Maron, L.; Walensky, J. R. Divergent uranium- versus phosphorus-based reduction of Me_3SiN_3 with steric modification of phosphido ligands. *Chem. Sci.* **2020**, *11*, 5830−5835.
(74) Weiss, C. J.; Marks, T. J. Organo-f-element catalysts for efficient and highly selective hydroalkoxylation and hydrothiolation. *Dalton Trans.* **2010**, *39*, 6576−6588.
(75) Zheng, P.; Hong, J.; Liu, R.; Zhang, Z.; Pang, Z.; Weng, L.; Zhou, X. Synthesis and Reactivities of Guanidinate Dianion Complexes of Heterobimetallic Lanthanide−Lithium Cp_2 Ln-$[(CyN)_2CNPh]Li(THF)_3$. *Organometallics* **2010**, *29*, 1284−1289.
(76) Watt, F. A.; Krishna, A.; Golovanov, G.; Ott, H.; Schoch, R.; Wölper, C.; Neuba, A. G.; Hohloch, S. Monoanionic Anilidophosphine Ligand in Lanthanide Chemistry: Scope, Reactivity, and Electrochemistry. *Inorg. Chem.* **2020**, *59*, 2719−2732.
(77) Garner, M. E.; Arnold, J. Reductive Elimination of Diphosphine from a Thorium−NHC−Bis(phosphido) Complex. *Organometallics* **2017**, *36*, 4511−4514.
(78) Kühl, O. *Phosphorus-31 NMR Spectroscopy*; Springer Berlin Heidelberg: Berlin, Heidelberg, 2009.
(79) Vilanova, S. P.; Alayoglu, P.; Heidarian, M.; Huang, P.; Walensky, J. R. Metal−Ligand Multiple Bonding in Thorium Phosphorus and Thorium Arsenic Complexes. *Chem. - Eur. J.* **2017**, *23*, 16748−16752.
(80) Romanov, A. S.; Becker, C. R.; James, C. E.; Di, D.; Credgington, D.; Linnolahti, M.; Bochmann, M. Copper and Gold Cyclic (Alkyl)(amino)carbene Complexes with Sub-Microsecond Photoemissions: Structure and Substituent Effects on Redox and Luminescent Properties. *Chem. - Eur. J.* **2017**, *23*, 4625−4637.
(81) Gernert, M.; Müller, U.; Haehnel, M.; Pflaum, J.; Steffen, A. A Cyclic Alkyl(amino)carbene as Two-Atom π-Chromophore Leading to the First Phosphorescent Linear CuI Complexes. *Chem. - Eur. J.* **2017**, *23*, 2206−2216.
(82) Di, D.; Romanov, A. S.; Yang, L.; Richter, J. M.; Rivett, J. P. H.; Jones, S.; Thomas, T. H.; Abdi Jalebi, M.; Friend, R. H.; Linnolahti, M.; Bochmann, M.; Credgington, D. High-performance light-emitting diodes based on carbene-metal-amides. *Science* **2017**, *356*, 159−163.
(83) Romanov, A. S.; Di, D.; Yang, L.; Fernandez-Cestau, J.; Becker, C. R.; James, C. E.; Zhu, B.; Linnolahti, M.; Credgington, D.; Bochmann, M. Highly photoluminescent copper carbene complexes based on prompt rather than delayed fluorescence. *Chem. Commun.* **2016**, *52*, 6379−6382.
(84) Shi, S.; Jung, M. C.; Coburn, C.; Tadle, A.; Sylvinson, M. R. D.; Djurovich, P. I.; Forrest, S. R.; Thompson, M. E. Highly Efficient Photo- and Electroluminescence from Two-Coordinate Cu(I) Complexes Featuring Nonconventional N-Heterocyclic Carbenes. *J. Am. Chem. Soc.* **2019**, *141*, 3576−3588.
(85) Hamze, R.; Peltier, J. L.; Sylvinson, D.; Jung, M.; Cardenas, J.; Haiges, R.; Soleilhavoup, M.; Jazzar, R.; Djurovich, P. I.; Bertrand, G.; Thompson, M. E. Eliminating nonradiative decay in Cu(I) emitters: 99% quantum efficiency and microsecond lifetime. *Science* **2019**, *363*, 601−606.
(86) Li, J.; Wang, L.; Zhao, Z.; Li, X.; Yu, X.; Huo, P.; Jin, Q.; Liu, Z.; Bian, Z.; Huang, C. Two-Coordinate Copper(I)/NHC Complexes: Dual Emission Properties and Ultralong Room-Temperature Phosphorescence. *Angew. Chem., Int. Ed.* **2020**, *59*, 8210−8217.
(87) Jazzar, R.; Soleilhavoup, M.; Bertrand, G. Cyclic (Alkyl)- and (Aryl)-(amino)carbene Coinage Metal Complexes and Their Applications. *Chem. Rev.* **2020**, *120*, 4141−4168.
(88) Bertrand, B.; Romanov, A. S.; Brooks, M.; Davis, J.; Schmidt, C.; Ott, I.; O'Connell, M.; Bochmann, M. Synthesis, structure and cytotoxicity of cyclic (alkyl)(amino) carbene and acyclic carbene complexes of group 11 metals. *Dalton Trans.* **2017**, *46*, 15875−15887.
(89) Frey, G. D.; Dewhurst, R. D.; Kousar, S.; Donnadieu, B.; Bertrand, G. Cyclic (Alkyl)(amino)carbene Gold(I) complexes: A Synthetic and Structural Investigation. *J. Organomet. Chem.* **2008**, *693*, 1674−1682.
(90) Romanov, A. S.; Bochmann, M. Gold(I) and Gold(III) Complexes of Cyclic (Alkyl)(amino)carbenes. *Organometallics* **2015**, *34*, 2439−2454.
(91) Romanov, A. S.; Bochmann, M. Synthesis, structures and photoluminescence properties of silver complexes of cyclic (alkyl)-(amino)carbenes. *J. Organomet. Chem.* **2017**, *847*, 114−120.
(92) Jurkauskas, V.; Sadighi, J. P.; Buchwald, S. L. Conjugate reduction of α,β-unsaturated carbonyl compounds catalyzed by a copper carbene complex. *Org. Lett.* **2003**, *5*, 2417−2420.
(93) de Frémont, P.; Scott, N. M.; Stevens, E. D.; Nolan, S. P. Synthesis and Structural Characterization of N-Heterocyclic Carbene Gold(I) Complexes. *Organometallics* **2005**, *24*, 2411−2418.
(94) Braunschweig, H.; Ewing, W. C.; Kramer, T.; Mattock, J. D.; Vargas, A.; Werner, C. Organometallic Probe for the Electronics of Base-Stabilized Group 11 Metal Cations. *Chem. - Eur. J.* **2015**, *21*, 12347−12356.
(95) Griffiths, M. B. E.; Koponen, S. E.; Mandia, D. J.; McLeod, J. F.; Coyle, J. P.; Sims, J. J.; Giorgi, J. B.; Sirianni, E. R.; Yap, G. P. A.; Barry, S. T. Surfactant Directed Growth of Gold Metal Nanoplates by Chemical Vapor Deposition. *Chem. Mater.* **2015**, *27*, 6116−6124.
(96) Johnson, M. W.; Shevick, S. L.; Toste, F. D.; Bergman, R. G. Preparation and reactivity of terminal gold(i) amides and phosphides. *Chem. Sci.* **2013**, *4*, 1023−1027.
(97) Lavallo, V.; Canac, Y.; Präsang, C.; Donnadieu, B.; Bertrand, G. Stable cyclic (alkyl)(amino)carbenes as rigid or flexible, bulky, electron-rich ligands for transition-metal catalysts: a quaternary carbon atom makes the difference. *Angew. Chem., Int. Ed.* **2005**, *44*, 5705−5709.
(98) Neogrády, P.; Kellö, V.; Urban, M.; Sadlej, A. J. Ionization Potentials and Electron Affinities of Cu, Ag, and Au: Electron Correlation and Relativistic Effects. *Int. J. Quantum Chem.* **1997**, *63*, 557−565.
(99) Gaillard, S.; Nun, P.; Slawin, A. M. Z.; Nolan, S. P. Expeditious Synthesis of $[Au(NHC)(L)]^+$ (NHC = N-Heterocyclic Carbene; L =

https://dx.doi.org/10.1021/acs.inorgchem.0c01971
Inorg. Chem. 2020, 59, 13621−13631

Phosphine or NHC) Complexes. *Organometallics* **2010**, *29*, 5402−5408.
(100) Lazreg, F.; Slawin, A. M. Z.; Cazin, C. S. J. Heteroleptic Bis(N-heterocyclic carbene)Copper(I) Complexes: Highly Efficient Systems for the [3 + 2] Cycloaddition of Azides and Alkynes. *Organometallics* **2012**, *31*, 7969−7975.
(101) Soleilhavoup, M.; Bertrand, G. Cyclic (alkyl)(amino)carbenes (CAACs): Stable Carbenes on the Rise. *Acc. Chem. Res.* **2015**, *48*, 256−266.

https://dx.doi.org/10.1021/acs.inorgchem.0c01971
Inorg. Chem. 2020, 59, 13621−13631